

Research Article Open Access

Human Induced Pluripotent Stem Cells Derived from A Patient with Sporadic Alzheimer's Disease Exhibit Altered Neuronal Proliferative Capacity

Chung H1, Lie KH1, Lin RCY2,3, Sachdev PS1 and Sidhu KS11

- ¹Centre for Healthy Brain Ageing (CHeBA), School of Psychiatry, Faculty of Medicine, University of New South Wales, NSW, Australia
- ²Asbestos Diseases Research Institute, Sydney, Australia
- ³Ramaciotti Centre for Genomics and School of Biotechnology and Biomolecular Sciences, University of New South Wales, Sydney, Australia

*Corresponding author: Sidhu KS, Centre for Healthy Brain Ageing (CHeBA), School of Psychiatry University of New South Wales, Randwick, NSW 2052 Australia, Tel: +61401766055, E-mail: k.sidhu@unsw.edu.au Citation: Chung H, Lie KH, Lin RCY, Sachdev PS, Sidhu KS (2015) Human Induced Pluripotent Stem Cells Derived from A Patient with Sporadic Alzheimer's Disease Exhibit Altered Neuronal Proliferative Capacity. J stem cells clin pract 1(1): 106

Abstract

We generated two hiPSC clones from a patient with sporadic late-onset Alzheimer's disease (AD-iPSCs), which expressed typical undifferentiated markers and passed standard pluripotency assays. Genome-wide microarray analysis revealed that AD-iPSCs were highly similar to control hiPSCs and hESCs, albeit with some noticeable differences in few genes, viz.: DNAJC15, GRPR, NAIP and SNORD116-18. Several other biomarkers were differentially expressed in AD-iPSC clones which have been implicated in memory impairment and AD. Furthermore, well characterized familial (APP, PSEN1, PSEN2) and non-familial (A2M, APOE, GAP43, MAOA, MPO, PLAT, PLAU, SORL1, SNCA) AD-associated genes exhibited different expression patterns but were largely reset upon reprogramming into a pluripotent state. AD-iPSC clones could efficiently form neuroprogenitors via rosette formation but one of the two AD-iPSC clones exhibited a lower proliferation rate as determined by EdU incorporation assays. Further analysis revealed this lower proliferation was due to an increase in apoptotic gene expression. The data suggest that hiPSCs could be good candidates for AD modeling and may represent an *in vitro* alternative to studying disease mechanisms, drug discovery and toxicological studies. Further studies are required to ascertain the significance of the resetting of disease specific genes caused by reprogramming as seen in this study.

Keywords: Alzheimer's disease; Pluripotent stem cells; pluripotency assays; AD-iPSCs

Introduction

Alzheimer's disease (AD) is a neurodegenerative disorder associated with the loss of neurons that are vital for memory and other cognitive functions [1]. Current treatments have limited benefits and with the number of affected people expected to quadruple by 2050, effective therapies are required. Our current understanding of AD comes from diverse sources including neuronal cell lines [2-5], transgenic rodent models [6,7] and primary neuronal cell cultures derived from them [8]. However, candidate proteins known to be involved in the disease pathology may exhibit species-specific biochemical and functional characteristics, thereby providing only an imperfect human representation. Therefore it is important to develop alternative models that correctly recapitulate the complex pattern of proteins in human AD.

Pluripotent stem cells may be good 'disease models' because of their unique capacity to differentiate and self-renew and their developmental representation of early stages of life. Generation of disease-specific human embryonic stem cell (hESC) lines from pre-implantation genetic diagnosed (PGD) embryos is limited by their availability. The genetic engineering of existing hESC lines is also possible but these present technical difficulties. The recent production of induced pluripotent stem cells (iPSCs) offers a potential solution as these cells can be produced from patient skin with a simple transduction of four genes (*OCT4*, *KLF4*, *SOX2*, *CMYC*) [9]. Diseased-specific iPSCs have been generated for several disorders including Spinal muscular atrophy, Long-QT syndrome and Huntington's disease as reviewed by Sidhu [10], all of which demonstrated genetic and phenotypic differences in the relevant differentiated cell type(s) when compared to control healthy iPSCs derived from un/related individuals. These and other recent developments in sporadic cases of Alzheimer's disease [11,12] provide unprecedented advantages for drug discovery and providing further insight into disease etiology.

AD is generally diagnosed by cognitive impairment/dysfunction and functional impairment, with an increasing emphasis on biomarkers, and ultimately through histological analysis of *post mortem* brains. Most patients with AD have a late-onset sporadic form of the disease. Environmental factors, vascular risk factors, presence of Apolipoprotein $\varepsilon 4$ (*APOE4*) allele, and some other genetic polymorphisms all greatly increase a person's susceptibility to sporadic AD, as reviewed by Taupin [13].

In the present study we have generated AD-iPSC clones from a sporadic female AD patient with strong clinical symptoms and performed a genome-wide transcriptome analysis with control pluripotent cells. Interestingly, several potential biomarkers impli-

cated in memory impairment and AD were differentially expressed. This suggests that AD-iPSCs may provide an alternative *in vitro* model to study the underlying mechanisms of AD.

Materials and methods

Ethics Statement

This study was conducted in accordance with the University of New South Wales (UNSW), Human Research Ethics Committee (HREC) approvals (HREC # 08037).

Cell culture and generation of AD-iPSCs

Human dermal fibroblasts were isolated from a punch skin biopsy from the female patient clinically diagnosed sporadic case of Alzheimer's disease with APOE $\alpha 4/4$. Fibroblasts were cultured in DMEM media supplemented with 10% FBS, Penicillin/streptomycin and Glutamax for 2-3 weeks. At passage 2-5, 100,000 fibroblasts were transduced with a polycistronic lentiviral vector encoding for genes; *OCT4*, *KLF4*, *SOX2*, *CMYC* under a constitutive promoter [14]. At day 5, transduced cells were harvested and seeded onto irradiated human fetal fibroblast feeder layers in hESC maintenance media (KO-DMEM supplemented with 20% SR, Glutamax, Penicillin/streptomycin, non-essential amino acids, Insulin transferrin selenium, β -mecaptoethanol). Daily media changes were performed using hESC maintenance media supplemented with 10 ng/ml bFGF. Control iPSCs were derived in a similar fashion using human fetal fibroblasts. Control (Co-) and AD-iPSCs were later transferred to a feeder-free system using hESC-qualified MatrigeTM(BD Biosciences) coated plates and mTeSRTM1 media (StemCell Technologies), according to manufacturer's protocol. All reagents were purchased from Life Technologies unless otherwise stated.

Neuroprogenitor induction

Neuroprogenitor differentiation was carried out following [15] slight modifications to Zhang's *et al.* protocol [16]. Briefly, confluent wells of pluripotent stem cells were subjected to 1 mg/ml dispase treatment for 20-30 min at 37 °C (or until intact colonies 'lifted' off) and further cultured for 4 days in mTeSRTM1 media in low adherent culture plates. Spherical aggregates were cultured for a further 3 days in neural induction media (DMEM/F12 supplemented with N2 (1%), non-essential amino acids and heparin). Aggregates were then transferred to laminin-coated (\sim 20 µg/ml) plates for a further 8 days. Partial media changes were performed every other day. Neural rosette-like structures were observed at the end of 15 days induction and subjected to 1 mg/ml dispase treatment for 5-10 min. Gentle trituration allowed the dislodgement of the rosette-like structures and the cell suspension was transferred to low adherent culture plates in neural maintenance media (neural induction media supplemented with B27 (1%) and 20 ng/ml bFGF). After overnight culture, floating aggregates were transferred to a new well, hence selecting out the attached neuroepithelial cells. Floating aggregates were propagated as neurospheres and were passaged on a 2-3 weekly basis by mechanical dissociation. Partial media changes were performed every other day.

Transcriptomic profiling

100 ng of total RNA from hESCs and iPSCs were labeled and hybridized onto Affymetrix Human GeneChip® Gene 1.0 ST arrays (Santa Clara, USA) according to the manufacturer's instructions at the Ramaciotti Centre for Genomics (UNSW, Australia). RMA normalized data [17] was subjected to one-way ANOVA to look for differential gene expression between cell lines (Partek Genome Suite v6.5). A False Discovery Rate (FDR) of 0.05 was used. Candidate genes were functionally annotated according to Gene Ontology (GO) terms [18].

Hierarchical clustering was carried out to look for possible co-regulation of significant differentially expressed candidate genes based on Euclidean and complete linkage distances using MeV 4.6.2 [19]. Further analysis to highlight Alzheimer's disease related genes was carried out by obtaining the gene list from SABiosciences-curated pathways (Maryland, USA).

Gene expression

Total RNA was extracted using TRIzol® and 1 μ g was reverse transcribed to cDNA using SuperScript® III kit with random hexamers. Genes of interest were quantitatively detected using SsoFast™ EvaGreen® supermix (BioRad) and relative expression calculated using Pfaffl's methods [20]. All reagents were purchased from Life Technologies following manufacturer's instructions unless stated otherwise. Biological triplicates were used.

Immunocytochemistry staining

Cell samples were fixed in 4% paraformaldehyde (Sigma-Aldrich) for 20 min, permeablized with 0.1% Triton X-100/PBS for 10 min and blocked with 2% BSA/PBS for 1 h. Cell samples were stained with appropriate primary antibodies in blocking solution overnight at 4 °C and AlexoFluor* conjugated secondary antibodies (Life Technologies) for 30 min at room temperature. Cells were counterstained with DAPI (Life Technologies). Primary antibodies: SOX17 (R&D Systems), OCT4, NANOG, SSEA4, TRA160 and SMA (Abcam), β III tubulin (Covance), NESTIN (Millipore), PAX6 and SOX1 (Santa Cruz).

Results

Characterization of AD-iPSCs

Using our previously optimized procedure [14] two iPSC clones were established and designated as Alzheimer's disease-specific lines, i.e. ALZ1 and ALZ7, and these were subcultured on a 5-7 day basis using TrypLE Select for 5-10 passages before being transferred to a feeder-free system consisting of MatrigelTM coated plates and mTeSRTM1 medium [21]. Colonies of AD-iPSCs were morphologically indistinguishable from control (Co) iPSC and hESCs (Figure 1A).

Further characterization revealed that AD-iPSCs were genetically and phenotypically indistinguishable from control hESC/hiPSCs. Hypomethylated *OCT4* promoter regions indicated successful reprogramming of fibroblasts (24.4% vs. 66.7%, Figure 1B). Using immunofluorescence staining, feeder-free cultures of AD-iPSCs typically expressed undifferentiated pluripotent markers *OCT4*, *NANOG*, *SSEA4* and *TRA160* (Figure 1C). Quantitative gene expression analyses of pluripotency-associated genes were not significantly different across pluripotent cell lines. In contrast, parental fibroblasts (AD-Fib) expressed extremely low levels of *NANOG*, *OCT4*, *SOX2* and *GDF3*, but had similar levels of *CMYC* and *KLF4* expression (Figure 1D). Furthermore, extended feeder-free culture showed no chromosomal abnormalities in ALZ1/ALZ7 as determined by standard G-banding karyotypic analysis (Figure 1E).

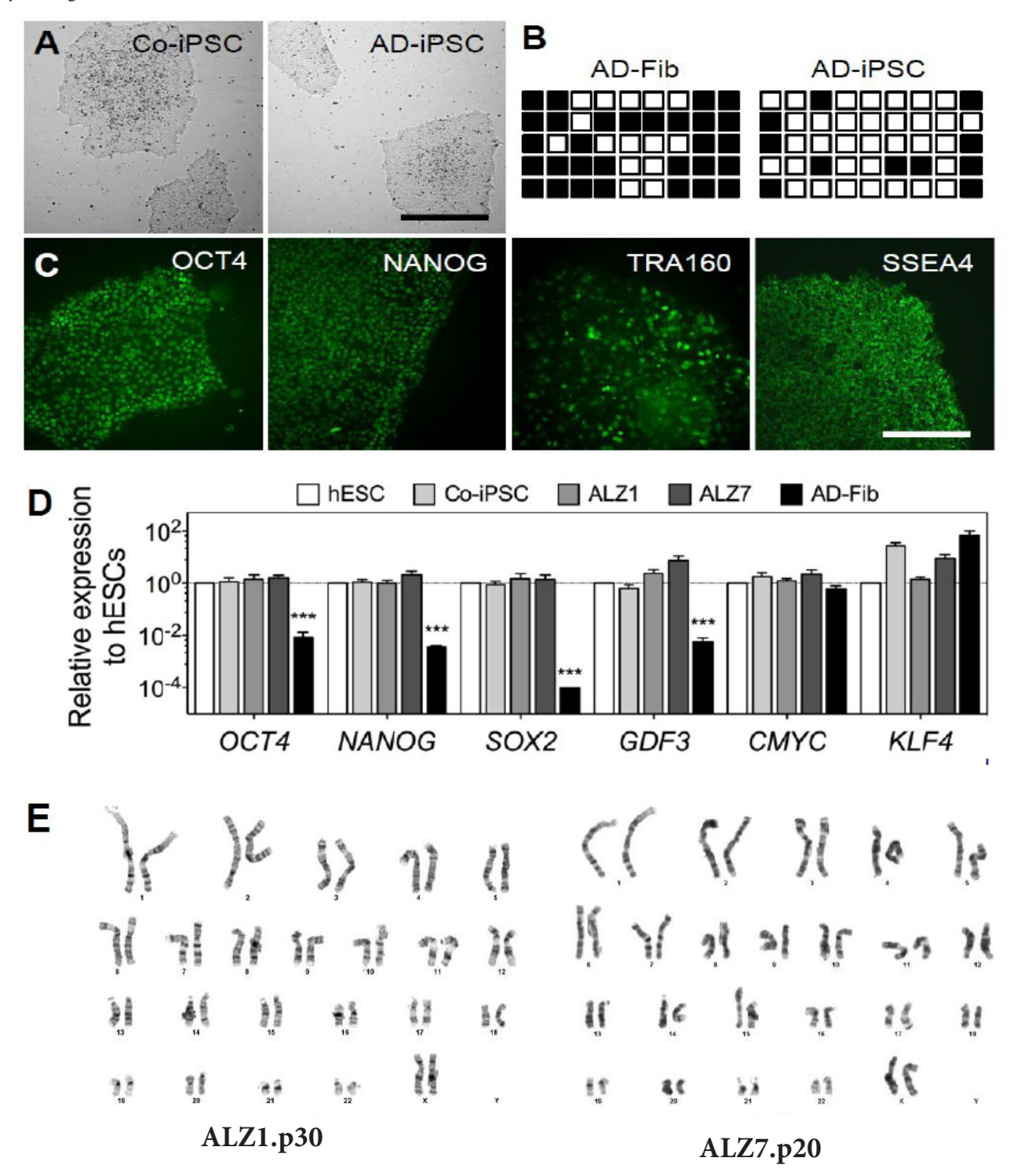


Figure 1: Characterization of Alzheimer's disease specific hiPSCs (AD-iPSCs). A) Colony morphologies of control and diseased hiPSCs under feeder-free conditions. Scale = $500 \mu m$. B) OCT4 promoter DNA methylation analysis using bisulfite sequencing. (Open squares: Unmethylated, closed squares: Methylated). C) Immunofluorescence staining of typical undifferentiated nuclear/surface markers, OCT4, NANOG, TRA160, SSEA4. Scale = $200 \mu m$. D) Gene expression analyses of pluripotency related genes using quantitative PCR. *** P < 0.0005. E) Standard G-banding karyotypic analysis of AD-iPSCs after extended propagation under feeder-free conditions

Pluripotency of AD-iPSCs was examined through *in vitro* embryoid body formation and *in vivo* teratoma formation assays. Cells and tissue structures generated were representative of the three embryonic germ layers, respectively (Figure 2A-C). DNA fingerprinting analysis confirmed the genetic identity of AD-iPSCs as being derived from AD-Fib and not from cross-contamination with other cell lines (Figure S1).

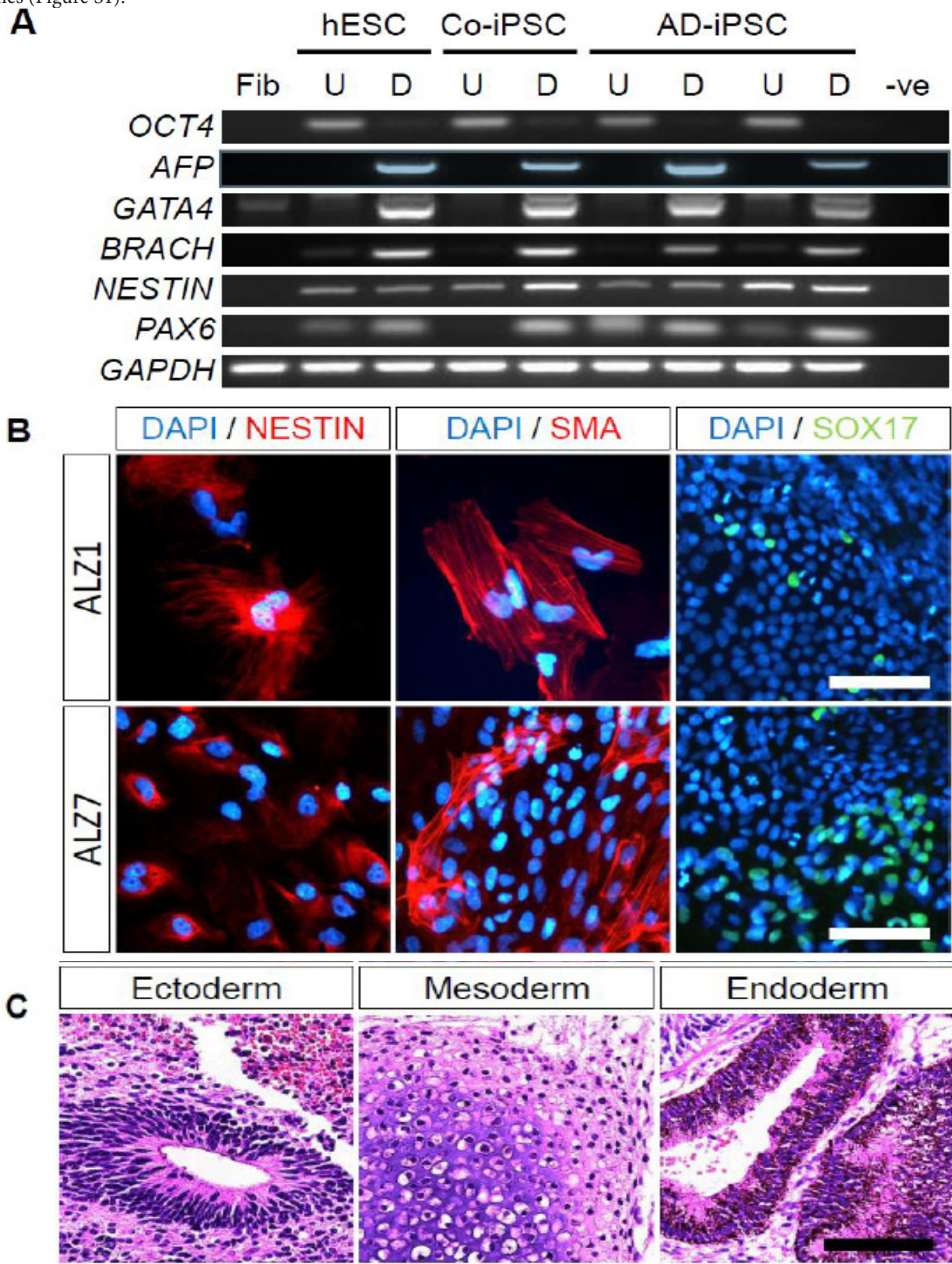


Figure 2: *In vitro* **and** *in vivo* **analysis of pluripotency of AD-iPSCs. A)** Gene expression analysis of early lineage markers in the undifferentiated (U) and embryoid body differentiated (D) states of pluripotent cell lines. OCT4: Pluripotency, AFP & GATA4: Endoderm, BRACHYURY (BRACH): Mesoderm and NESTIN & PAX6: Ectoderm. **B)** Immunofluorescence staining of early lineage markers after *in vitro* differentiation induced by embryoid body attachment in FBS containing media. **C)** *In vivo* teratoma formation assays were performed by intratesticular injection of AD-iPSCs into SCID mice. Representative tissues of the 3 embryonic lineages were observed. Scale = 50 μm

Transcriptomic analysis of AD-iPSCs

The transcriptome of AD-iPSCs was similar to Co-iPSCs and hESCs, as determined by whole-genome transcript analysis using Affymetrix Human Gene 1.0 ST arrays. Scatterplots and correlation coefficients revealed that on the 33,297 transcripts, AD-iPSCs, Co-iPSCs and hESCs were highly correlated with each other whereas minimal correlation was observed between fibroblasts and pluripotent cells (Figure S2A-B). A heat map was generated based on 4,532 genes that were differentially expressed (False discovery rate (FDR)-corrected P value < 0.05 and fold change $> \pm 2$), between fibroblast and pluripotent cell populations (Figure S2C). Overall, this indicated that AD-iPSCs were highly similar to Co-iPSCs and hESCs in terms of global gene expression.

However, some genes were differentially expressed between control (hESC/Co-iPSC) and disease (AD-iPSC) pluripotent cell populations. Based on a FDR-corrected P value < 0.05 and fold change > ±1.3, a total of 335 and 160 genes were further analyzed in [AD-iPSC vs. Co-iPSC] and [AD-iPSC vs. hESC], respectively. By conducting gene ontology (GO) enrichment analysis, genes with common biological function were ranked based on the number of times a gene was enriched for a particular function. Immune response and neuronal developmental GO terms were significantly enriched (i.e. enrichment score > 3) in AD-iPSCs, whereas cell junction assembly and maintenance of DNA repeat element GO terms were enriched in control cells (Figure S3A-B). Furthermore, 5 genes exhibited > 3 fold change between AD-iPSCs and hESCs/Co-PSCs; DNAJC15, GRPR, HLA-DQB1, NAIP and SNORD116-18 (Figure 3A-B). Both DnaJ (Hsp40) homolog, subfamily C, member 15 (DNAJC15) and Major histocompatibility complex, class II, DQ beta 1 (HLA-DQB1) have been implicated with functions of immunological response and these genes were highly expressed in AD-iPSCs, which was consistent with GO enrichment analysis (Figure S3). Interestingly, gastrin releasing

peptide receptor (*GRPR*) was also significantly upregulated in AD-iPSCs and has been implicated in AD and other neurological disorders [22]. In contrast, small nucleolar RNA, C/D box 116 (*SNORD116-18*) and neuronal apoptosis inhibitory protein (*NAIP*) were significantly downregulated in AD-iPSCs

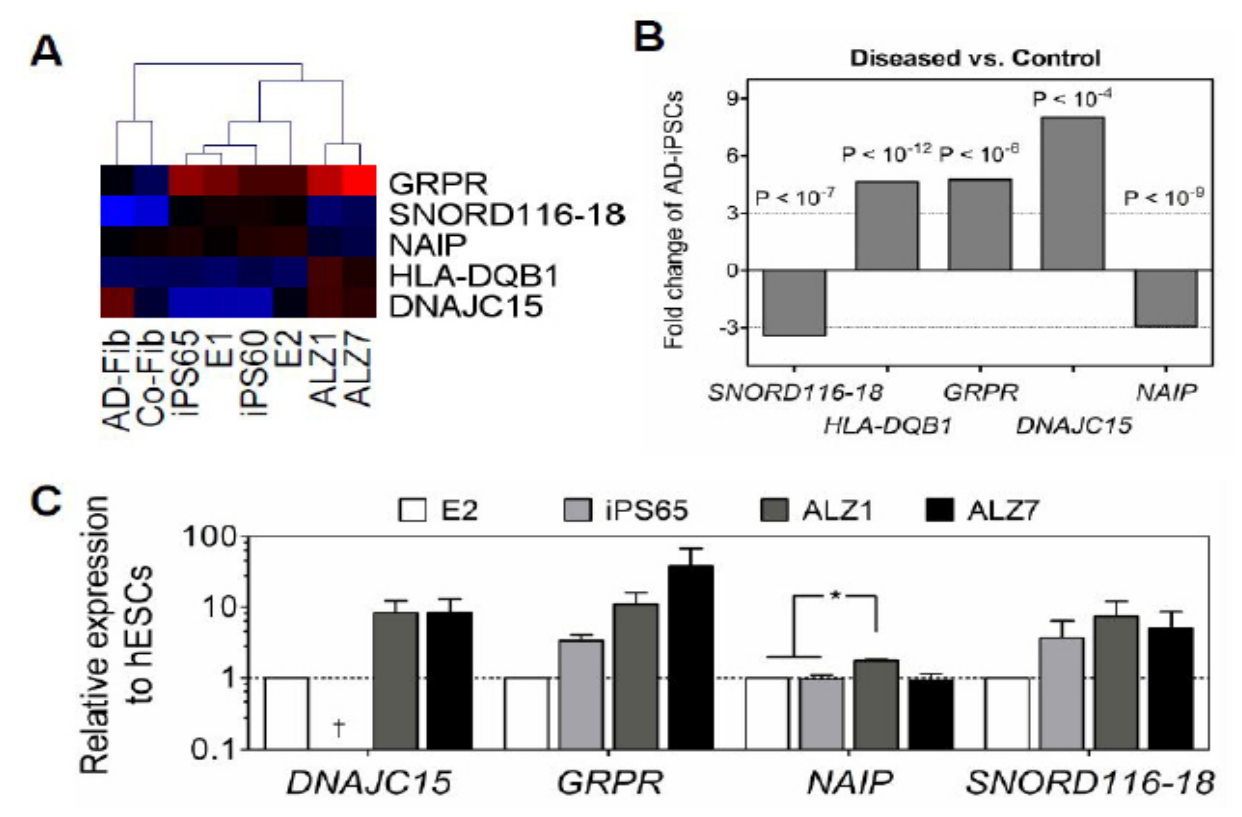


Figure 3: Differentially expressed genes of control and disease pluripotent cell lines. A) Heatmap representation of the genes differentially expressed (Fold change $> \pm 3$) between control and diseased pluripotent lines. B) Graphical representation of the genes in A) based on microarray calculated values. Fold change displayed is representative of AD-iPSCs relatively to control cells. All values were significantly different. C) Gene expression analysis of four of these genes were confirmed by quantitative RT-PCR on E2 (hESC), iPS65 (Co-iPSC) and AD-iPSC lines. * P < 0.05

We further analyzed the expression of four of these genes using quantitative RT-PCR (qRT-PCR) (Figure 3C). Surprisingly, these genes were not significantly different from each control (E2, iPS65) or diseased (ALZ1, ALZ7) cell lines, which is in contrast to the microarray data. In fact, both *NAIP* and *SNORD116-18* were observed to have an opposite trend in gene expression. This was most probably due to the design of the primers used in qRT-PCR, which targeted multiple regions of *NAIP* (i.e. chr5:69404269-69404333, chr5:70279736-70279800 and chr5:70404622-70404686 on chromosome 5q13.2) and multiple 61 bp regions of the *SNORD116* gene cluster (chr15:25327944-25328004, chr15:253328764-25328824, chr15:25330561-25330621, chr15:25331703-25331763, chr15:25332838-25332898, chr15:25333980-25334040, chr15:25335099-25335159 on chromosome 15q11-13).

Furthermore, well characterized familial AD-associated genes (*APP, PSEN1, PSEN2*) [23,24] and non-familial (*A2M, APOE, GAP43, MAOA, MPO, PLAT, PLAU, SORL1, SNCA*) [13,25-27], exhibited different expression patterns, as determined by the microarrays but were largely reset upon reprogramming into a pluripotent state (Figure S4).

Differentiation of AD-iPSCs into neuroprogenitors

We next examined whether AD-iPSCs could develop into neuronal lineages by following a slightly modified neural induction protocol [16]. By day 10 of neural induction, PAX6+ and SOX1+ cells were apparent among the attached clusters (data not shown). We were able to generate neurospheres in hESC, Co-iPSC and AD-iPSC populations through mechanical dissociation of neural rosettes formed at the end of a 15 day induction period (Figure 4A). Immunofluorescence analysis indicated that neuroprogenitors derived from control and disease cell lines stained positive for *NESTIN*, *PAX6* and *SOX1* (Figure 4B). Gene expression analysis indicated that *NESTIN* and *SOX2* were minimally upregulated (< 10 fold), whereas PAX6 and SOX1 expression were upregulated up to \sim 10,000 fold (Figure 5A). *NANOG* was significantly downregulated in all neuroprogenitor lines as expected (P < 10-6) and was not significantly different between cell lines. Interestingly, only E2-neuroprogenitors exhibited statistically significant upregulated gene expression values in all neuronal genetic markers analyzed (P < 0.05), indicating that hESC differentiation protocols were more reproducible, whereas hiPSC differentiation were more variable (i.e. ranging between 100 to 10,000 fold). Overall, both protein expression and gene expression profiling in control and disease hiPSCs of neuronal markers (i.e. *NESTIN*, *PAX6*, *SOX1*, *SOX2*) indicated no significant differences in neuroprogenitor formation (Figure 5A-C).

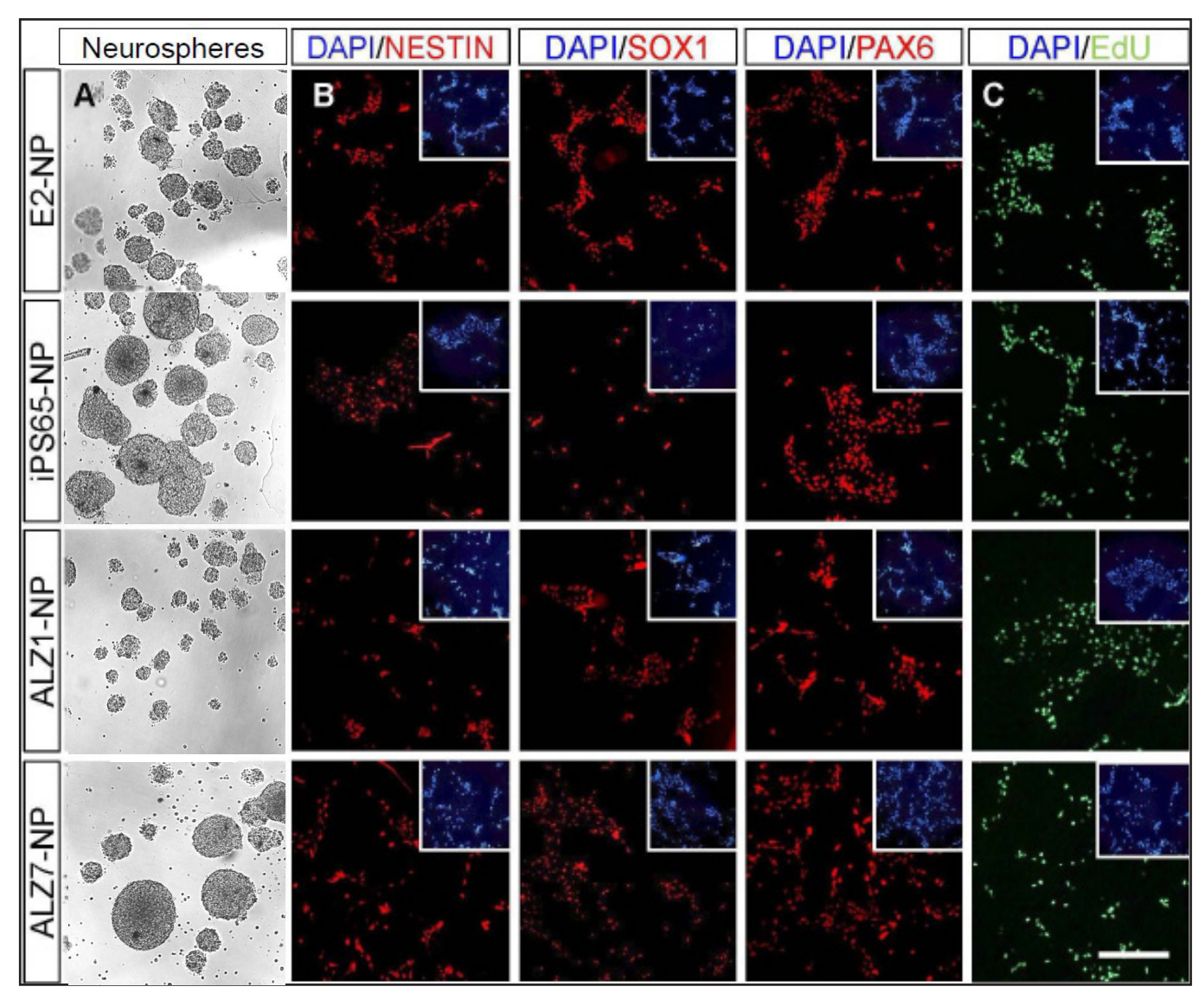


Figure 4: Neuroprogenitors derived from control and disease pluripotent cell lines. A) Morphological analysis of the neurospheres generated from dissecting out neural rosette-like structures. B) Neurospheres were dissociated into single cells and seeded onto laminin-coated dishes and stained positive for neural stem/progenitor markers; NESTIN, PAX6 and SOX1. C) EdU incorporation assays were performed to determine the proliferative capacity of these neuroprogenitors. Scale = $200 \, \mu m$

Neuroprogenitors or neural stem cells offer the potential to self-renew and differentiate into multiple neural/glial lineages. Therefore, we investigated the proliferation rate of AD-iPSC derived neuroprogenitors using 5-ethynyl-2′-deoxyuridine (EdU) incorporation assays. Interestingly, a significantly lower percentage of EdU+ cells were found in ALZ7-neuroprogenitors but not ALZ1-neuroprogenitors compared with control cells (Figure 4C, 5B). We next investigated whether this lower proliferation rate was due to an increase in apoptosis. Therefore we examined the expression of several key apoptosis-related genes. Amongst, *CASP3*, *CASP9*, *CDKN1A* (*p21*), *MDM2* and *TP53* (p53), only *TP53* and *CAPS9* genes were significantly different with control and ALZ1 derived neuroprogenitors (Figure 6A).

Furthermore, the 4 candidate genes *DNAJC15*, *GRPR*, *NAIP* and *SNORD116-18* isolated as being specific to AD-iPSCs, were also analyzed at the neuroprogenitor stages. Interestingly, none of the neuroprogenitor cell lines exhibited significant differences in gene expression (Figure 6B).

Discussion

Human iPSCs have been generated for many degenerative diseases, some of which displayed abnormal phenotypes following directed differentiation [28,29], while some were physiologically functional [30,31]. In the present study, we generated hiPSCs from a female sporadic AD patient and these cells were phenotypically indistinguishable from undifferentiated control hiPSCs and hESCs. Although global transcriptomic analysis revealed high similarity between disease and control pluripotent cells, there were a small number of genes that were differentially regulated, some of which have been implicated in neurological disorders.

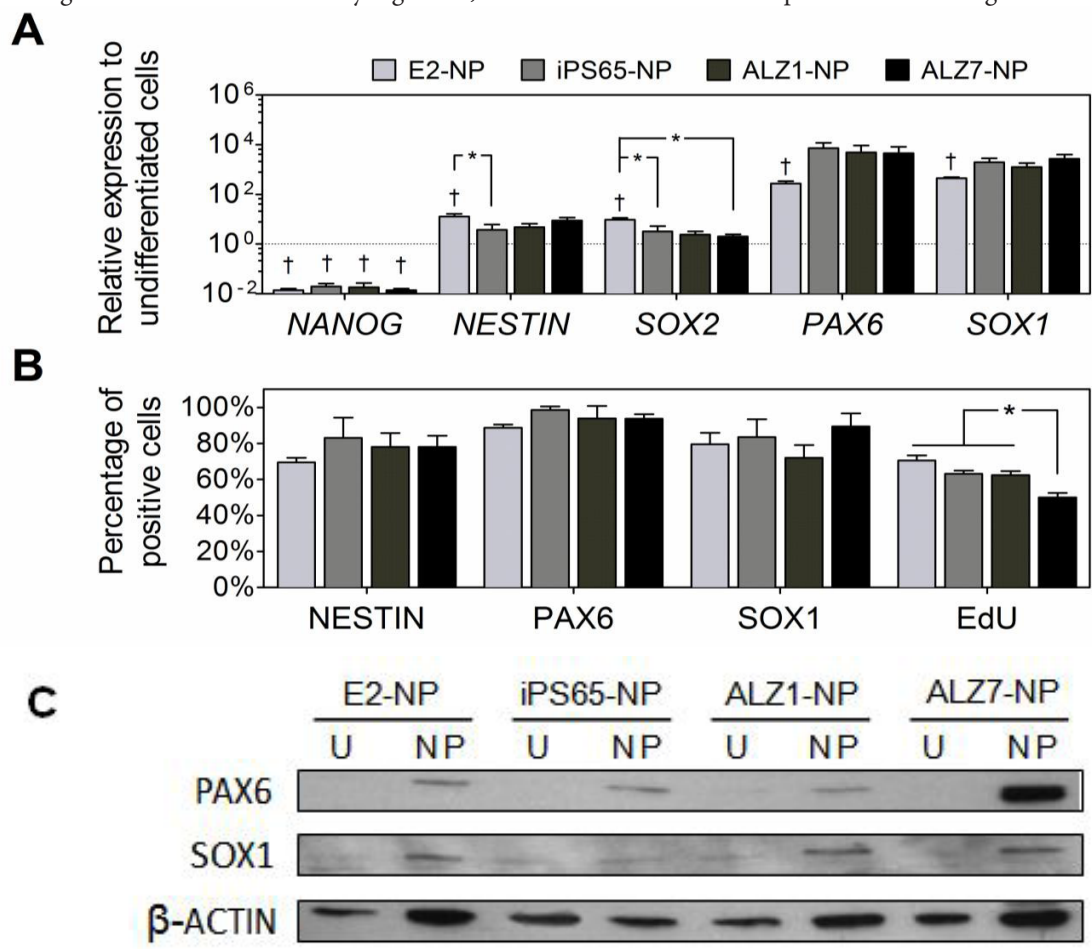


Figure 5: Analyses of AD-iPSC derived neuroprogenitors. A) Quantitative gene expression analysis of neuroprogenitors (NP). Markers include pluripotent (*NANOG*) and neural stem/progenitor genes (*NESTIN, SOX2, PAX6, SOX1*). **B)** Percentages of NESTIN⁺, PAX6⁺, SOX1⁺ and EdU⁺ cells represented in Figure 4B-C. Percentages were obtained from 9-12 random images from 3 independent biological experiments and calculated using pixel density using ImageJ software. *P < 0.05. **C)** Protein expression analysis of PAX6 and SOX1 using western blot. U: undifferentiated, NP: neuroprogenitor

Although neuronal apoptosis inhibitory protein (*NAIP*) was ~3 fold lower in AD-iPSCs than Co-iPSCs/hESCs (as determined by microarray analysis), qRT-PCR detected an equal amount of *NAIP* transcript in all undifferentiated cell lines. This was probably due to the design of the oligonucleotide primers which we later confirmed to amplify 2 other regions on the NAIP transcript. As the name suggests, NAIP is an anti-apoptotic protein and has been implicated in motor neuron apoptosis in spinal muscular atrophy [32]. Individuals with Down syndrome also exhibit decreased expression of NAIP in their cortex [33], and they are genetically predisposed to AD. Furthermore, NAIP is inversely related to paired helical filament-1 protein in brain tissue of AD individuals [34], which may indicate the presence of NFT pathology in non-familial AD-iPSCs.

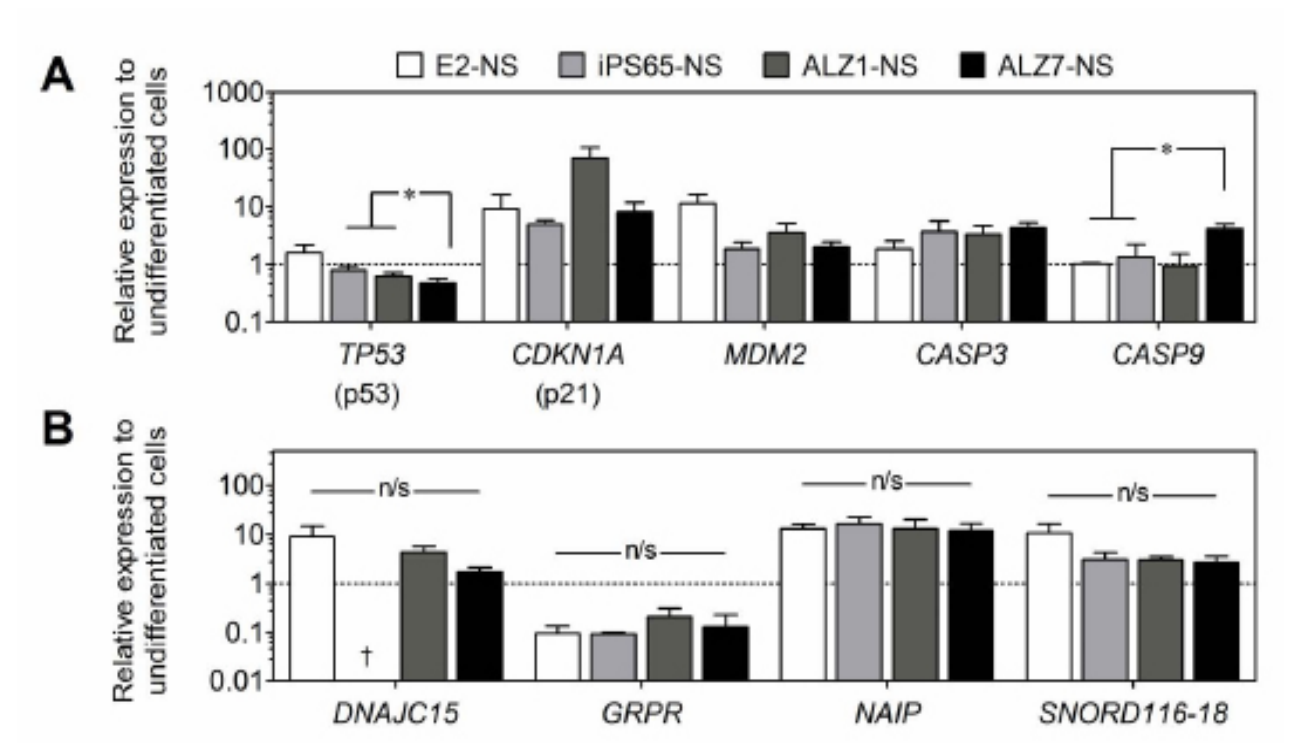


Figure 6: Mechanisms for the lower proliferation rate of AD-iPSC derived neuroprogenitors. A) Quantitative gene expression analysis of apoptosis-related genes; p53, p21, MDM2, CASP3 and CASP9. * P < 0.05. B) Analysis of candidate genes in neuroprogenitor lines that were differentially expressed between control and diseased pluripotent cell lines. n/s: non-significant. †No melt curves were present, indicating no PCR gene product

Gastrin releasing peptide receptor (GRPR) is a G-protein coupled receptor and has been extensively studied in cancers [35] and expressed in multiple regions of the central nervous system, including the hippocampus [36], a region important for episodic memory. It is increasingly evident that GRPR is associated with several neurological disorders, including AD, as reviewed in Roesler *et al.* [22]. The higher expression of *GRPR* in AD-iPSCs compared with their undifferentiated counterparts (~3 fold and ~10 fold in microarray and qPCR analysis, respectively), could arguably be due to an additional transcript copy on the X chromosome. However, since female hiPSC lines have been shown to retain their inactive X chromosome even after reprogramming into a pluripotent state [37], high *GRPR* levels may in fact be associated with AD. Furthermore, the increased expression may suggest susceptibility of receptor activation and subsequent long-term memory impairment [38], leading to AD-associated memory loss.

DNAJC15 (also known as *MCJ*, *DNAJD1*) is normally silenced in the majority of carcinoma cell lines via DNA hypermethylation and loss of *DNAJC15* causes resistance to chemotherapeutic agents *in vitro* [39,40]. Co-Fib readily expressed *DNAJC15*, but it was absent from Co-iPSCs and its neuroprogenitor derivatives. Extensive epigenetic remodeling takes place during somatic cell reprogramming [41,42], and the presence of multiple H3K27Ac regions (Histone 3 Lysine 27 acetylation, http://genome.ucsc.edu),

within the *DNAJC15* transcript indicates repressive (and also stable) epigenomic modification(s) to that particular genomic region, leading to gene silencing. Surprisingly, E1 but not E2 cell lines also exhibited this phenomenon. Therefore fetal derived hiPSCs (i.e. Co-iPSCs) may be more resistant to drug evaluations and subsequently may not be suitable candidates for high throughput screening (HTS) for drug discovery and/or toxicology studies.

Small nucleolar RNA, C/D box 116 (SNORD116) is a non-coding RNA region that resides in the SNRPN transcript and contains 29 tandem repeated copies of the SNORD116 gene (1-29, http://genome.ucsc.edu). Measuring SNORD116-18 was difficult since the qPCR primers targeted multiple regions within SNORD116 and subsequently contradicted results from the microarray analysis. Though results were inconclusive, SNORD116 was reportedly expressed at low levels in hiPSCs derived from Prader-Willi syndrome patients – a neurological disorder caused by gene deletions [43]. This indicates a possible link between AD and Prader-Willi syndrome. Whether SNORD116-18 is involved with neurological diseases or bears a consequence of somatic cellular reprogramming, remains to be defined.

Control and disease cells could differentiate into neuroprogenitors, however variable gene expression patterns were observed in our hiPSC-derived neuroprogenitors, which were similar to other differentiation protocols [44-46]. This suggests that although hiPSCs can differentiate into multiple cell types like hESCs, their differential variability between cell lines (or in our case, within the same cell line) is statistically more prominent. Interestingly, one of the AD-iPSC-derived neuroprogenitor lines (i.e. ALZ7) exhibited a significantly lower proliferation rate when compared with other neuroprogenitor lines. With further analysis, we observed atypical *TP53* and *CASP9* gene expression, which was indicative of apoptosis. This may suggest potential apoptotic mechanism(s) are involved in the intermediate stages of AD, in addition to the ones reviewed by Crews and Masliah [47]. This would subsequently compromise neuronal development, correlating to individuals diagnosed with early onset non-familial AD.

Additionally, candidate genes we classified to be specific to sporadic AD based on differential expression (i.e. *DNAJC15, GRPR, NAIP, SNORD116-18*) were not significantly different between neuroprogenitor lines. Overall, differentiation of disease-specific hiPSCs into progenitor cell types was not significantly different to controls, and this was observed in several other studies [10,48]. Whether specific neuronal deficits or abnormal expression of our analyzed genes/proteins appear at a more terminal cell derivative (e.g. basal forebrain cholinergic neurons, glial) remains to be determined.

We have until now defined disease-specific hiPSCs based on the patient who donated the skin. For monogenic disorders, this is simple to characterize, but for complex diseases such as sporadic Alzheimer's, the disease specificity is defined by both patient phenotype and genotype, as with this study. Furthermore, environmental stressors and epigenetic influences also contribute to the difficulties in replicating faithfully in an *in vitro* model. Another limiting factor in the present study was the lack of an appropriate hiPSC control cell line. The ideal scenario would be to have unaffected sib-pair that can act as an internal control due to similar genetic background. To adequately study the pathophysiology of AD, multiple AD-iPSCs should be derived from patients with various clinical symptoms in order to reflect early/late onset and/or familial/sporadic versions of the disease.

Conclusions

We believe that the AD-iPSCs generated in this study is a representative disease-specific cell line, which will be an invaluable *in vitro* model to study the molecular mechanisms in AD and subsequently, for high throughput screening. However, before such application, it will be useful to further differentiate AD-iPSCs into mature neurons, such as cholinergic lineages of the basal forebrain as described elsewhere [15,49] to determine whether there is impairment during neuronal development. Because the two AD-iPSC lines exhibited contradicting outcomes, it is recommended that future disease modeling studies using hiPSCs should attempt to analyze three or more cell lines from any individual for accurate conclusions.

Supplementary Figures

STR	Cell line							
marker	hESC	Co-iPSC	AD-Fib	AD-iPSC1	AD-IPSC7			
D8S1179	11, 15	10, 12	8, 15	8, 15	8, 15			
D21S11	30	28, 30	30	30	30			
D7S820	11, 12	9, 11	8	8	8			
CSF1PO	12	10, 11	10, 12	10, 12	10, 12			
D3S1358	15, 16	14	16, 18	16, 18	16, 18			
TH01	6, 9	6, 9.3	9, 9.3	9, 9.3	9, 9.3			
D13S317	11, 12	12, 14	8, 10	8, 10	8, 10			
D16S539	11, 13	9, 11	11, 12	11, 12	11, 12			
D2S1338	19, 23	20, 24	19, 24	19, 24	19, 24			
D19S433	13, 14.2	14	13.2, 14	13.2, 14	13.2, 14			
νWA	14, 18	16, 17	18	18	18			
TPOX	8	8, 9	8, 10	8, 10	8, 10			
D18S51	13,15	12, 17	13, 20	13, 20	13, 20			
D5S818	12, 13	11	11	11	11			
FGA	18, 19	19, 23	20, 25	20, 25	20, 25			

Figure S1: DNA fingerprinting analysis of cell lines. Genetic identity of AD-iPSC lines was confirmed through examining 15 short tandem repeat (STR) alleles of parental fibroblasts and pluripotent cell lines. All cell lines were of female origin

Α		A	
-	٠	п	ı
	1	-	١

	Fibrol	blasts	hES	SCs	Co-il	PSCs	AD-il	PSCs
	AD-Fib	hFF3	E1	E2	iPS60	iPS65	ALZ1	ALZ7
AD-Fib							i.V	
hFF3	0.9734				Lliab	-		Low
E1	0.9116	0.9321			High			Low
E2	0.9167	0.9407	0.9886					
iPS60	0.9138	0.9380	0.9904	0.9948				
iPS65	0.9104	0.9320	0.9941	0.9902	0.9936			
ALZ1	0.9088	0.9306	0.9931	0.9900	0.9927	0.9947		
ALZ7	0.9203	0.9410	0.9921	0.9935	0.9925	0.9919	0.9915	

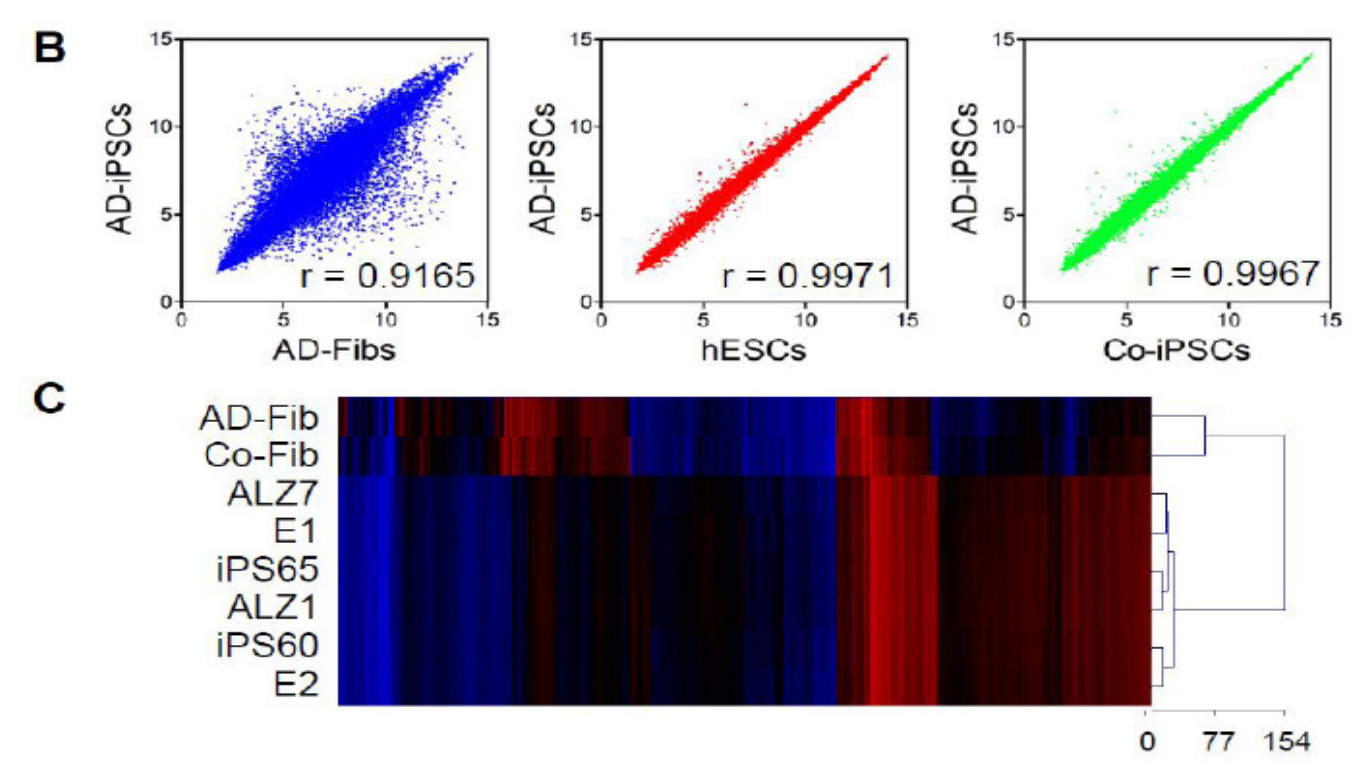


Figure S2: Global expression across all cell types. A) Pearson's correlation coefficients were determined between control and disease parental fibroblasts and pluripotent cell lines. B) Scatterplots of the mean signal intensity values of AD-Fibs, hESCs (E1, E2), Co-iPSCs (iPS60, iPS65) and AD-iPSCs (ALZ1, ALZ7) C) Heatmap/dendogram of the 4,532 differentially expressed genes between fibroblasts and pluripotent cell populations. These genes were selected based on a FDR-corrected P value < 0.05 and acquiring at least $> \pm 2$ fold change

Function (Up in AD-iPSCs)	Enrichment Score
Immune response	8.4
Cell growth	6.5
Protein processing	5.6
Stem cell maintenance	3.4
Central nervous system development	3.3
Organ development	3.2
S phase	3.1
Nerve growth factor processing	3.1
Function (Down in AD-iPSCs)	Enrichment Score
Growth hormone receptor signalling pathway	9.0
Cell junction assembly	7.5
Maintenance of DNA repeat elements	4.3
Insulin-like growth factor receptor signaling pathway	3.8
Phosphoinositide 3-kinase cascade	3.6
Neurotransmitter transport	3.6

Function (Up in AD-iPSCs)	Enrichment Score	
Protein tetramerization	5.2	
Immune response	4.9	
Response to stimulus	4.7	
Nucleotide biosynthetic process	4.0	
Dendrite development	4.0	
S phase	3.7	
Anatomical structure development	3.2	
Neuron differentiation	3.0	
Function (Down in AD-iPSCs)	Enrichment Score	
Maintenance of DNA repeat elements	5.1	013810
Cell junction assembly	4.1	ALZ7 ALZ1 PS60 PS65 E1
Sterol biosynthetic process	3.8	4 4 17 17
Mismatch repair	3.6	
DNA repair	3.5	

Figure S3: Differentially expressed genes between control and disease pluripotent lines. A) 335 genes were differentially expressed between AD-ipSCs vs. Co-iPSCs, and B) 160 genes between AD-iPSCs vs. hESCs. To determine overall biological functions, GO enrichment analysis was performed on genes that were up- or downregulated in a cell population. Functions with enrichment scores > 3 were considered significant. Heatmaps/dendograms were also generated for these two lists of genes, and surprisingly hESCs, Co-iPSCs and AD-iPSCs grouped separately from each other.

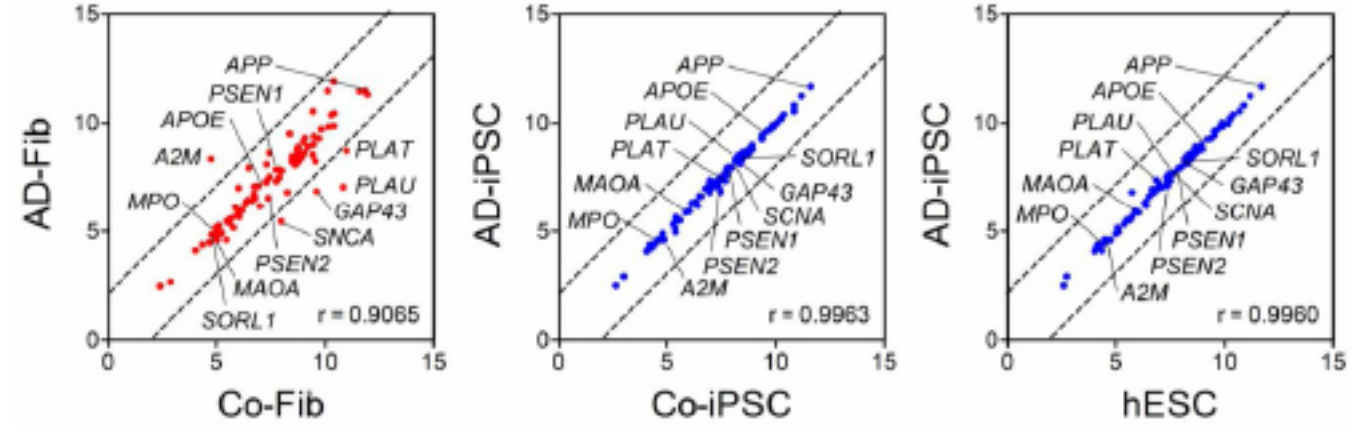


Figure S4: Analysis of Alzheimer's disease related genes. AD-associated genes (obtained from SABiosciences) were analyzed separately and both familial and non-familial AD-related genes were displayed in these scatterplots

References

- 1. Caselli RJ, Beach TG, Yaari R, Reiman EM (2006) Alzheimer's disease a century later. J Clin Psychiatry 67: 1784-800.
- 2. Neill D, Hughes D, Edwardson JA, Rima BK, Allsop D (1994) Human IMR-32 neuroblastoma cells as a model cell line in Alzheimer's disease research. J Neurosci Res 39: 482-93.
- 3. Trimmer PA, Swerdlow RH, Parks JK, Keeney P, Bennett JP, et al. (2000) Abnormal mitochondrial morphology in sporadic Parkinson's and Alzheimer's disease cybrid cell lines. Exp Neurol 162: 37-50.
- 4. Zhang Z, Drzewiecki GJ, Hom JT, May PC, Hyslop PA (1994) Human cortical neuronal (HCN) cell lines: a model for amyloid beta neurotoxicity. Neurosci Lett 177: 162-4.
- 5. Shaughnessy L, Chamblin B, McMahon L, Nair A, Thomas MB, et al. (2004) Novel approaches to models of Alzheimer's disease pathology for drug screening and development. J Mol Neurosci 24: 23-32.
- 6. Oddo S, Caccamo A, Shepherd JD, Murphy MP, Golde TE, et al. (2003) Triple-transgenic model of Alzheimer's disease with plaques and tangles: intracellular Abeta and synaptic dysfunction. Neuron 39: 409-21.
- 7. Tanzi RE (1995) A promising animal model of Alzheimer's disease. N Engl J Med 33: 1512-3.
- 8. Qiu Z, Naten DL, Liston JC, Yess J, Rebeck GW (2001) A novel approach for studying endogenous abeta processing using cultured primary neurons isolated from APP transgenic mice. Exp Neurol 170: 186-94.

- 9. Takahashi K, Tanabe K, Ohnuki M, Narita M, Ichisaka T, et al. (2007) Induction of pluripotent stem cells from adult human fibroblasts by defined factors. Cell 131: 861-72.
- 10. Sidhu KS (2011) New approaches for the generation of induced pluripotent stem cells. Expert Opin Biol Ther 11: 569-79.
- 11. Hossini AM, Megges M, Prigione A, Lichtner B, Toliat MR, et al. (2015) Induced pluripotent stem cell-derived neuronal cells from a sporadic Alzheimer's disease donor as a model for investigating AD-associated gene regulatory networks. BMC Genomics 16: 84.
- 12. Zhu XC, Tan L, Wang HF, Jiang T, Cao L, et al. (2015) Rate of early onset Alzheimer's disease: a systematic review and meta-analysis. Ann Transl Med 3: 38.
- 13. Taupin P (2009) Adult neurogenesis, neural stem cells and Alzheimer's disease: developments, limitations, problems and promises. Curr Alzheimer Res 6: 461-70.
- 14. Chung HC, Lin RC, Logan GJ, Alexander IE, Sachdev PS, et al. (2012) Human induced pluripotent stem cells derived under feeder-free conditions display unique cell cycle and DNA replication gene profiles. Stem Cells Dev 21: 206-16.
- 15. Lie, KH, Chung H, Sidhu KS (2012) Derivation, propagation and characterisation of neuroprogenitors from pluripotent stem cells (hESCs and hiPSCs) in Human Embryonic Stem Cells Handbook, Kursad Turksen Methods Mol Biol 873: 237-46.
- 16. Zhang XQ, Zhang SC (2010) Differentiation of neural precursors and dopaminergic neurons from human embryonic stem cells. Methods Mol Biol 584: 355-66.
- 17. Lin RC, Weeks KL, Gao XM, Williams RB, Bernardo BC, et al. (2010) PI3K (p110 alpha) protects against myocardial infarction-induced heart failure: identification of PI3K-regulated miRNA and mRNA. Arterioscler Thromb Vasc Biol 30: 724-32.
- 18. Ashburner M, Ball CA, Blake JA, Botstein D, Butler H, et al. (2000) Gene ontology: tool for the unification of biology. The Gene Ontology Consortium. Nat Genet 25: 25-9.
- 19. Saeed AI, Bhagabati NK, Braisted JC, Liang W, Sharov V, et al. (2006) TM4 microarray software suite. Methods Enzymol 411: 134-93.
- 20. Pfaffl MW (2001) A new mathematical model for relative quantification in real-time RT-PCR. Nucleic Acids Res 29: e45.
- 21. Ludwig TE, Bergendahl V, Levenstein ME, Yu J, Probasco MD, et al. (2006) Feeder-independent culture of human embryonic stem cells. Nat Methods 3: 637-46.
- 22. Roesler R, Henriques JA, Schwartsmann G (2006) Gastrin-releasing peptide receptor as a molecular target for psychiatric and neurological disorders. CNS Neurol Disord Drug Targets 5: 197-204.
- 23. Games D, Adams D, Alessandrini R, Barbour R, Berthelette P, et al. (1995) Alzheimer-type neuropathology in transgenic mice overexpressing V717F beta-amyloid precursor protein. Nature 373: 523-7.
- 24. Shen J, Bronson RT, Chen DF, Xia W, Selkoe DJ, et al. (1997) Skeletal and CNS defects in Presenilin-1-deficient mice. Cell 89: 629-39.
- 25. Saunders AM, Strittmatter WJ, Schmechel D, George-Hyslop PH, Pericak-Vance MA, et al. (1993) Association of apolipoprotein E allele epsilon 4 with lateonset familial and sporadic Alzheimer's disease. Neurology 43: 1467-72.
- 26. Rogaeva E, Meng Y, Lee JH, Gu Y, Kawarai T, et al. (2007) The neuronal sortilin-related receptor SORL1 is genetically associated with Alzheimer disease. Nat Genet 39: 168-77.
- 27. Ashford JW, Mortimer JA (2002) Non-familial Alzheimer's disease is mainly due to genetic factors. J Alzheimers Dis 4: 169-77.
- 28. Carvajal-Vergara X, Sevilla A, D'Souza SL, Ang YS, Schaniel C, et al. (2010) Patient-specific induced pluripotent stem-cell-derived models of LEOPARD syndrome. Nature 465: 808-12.
- 29. Marchetto MCN, Carromeu C, Acab A, Yu D, Yeo GW, et al. (2010) A model for neural development and treatment of Rett syndrome using human induced pluripotent stem cells. Cell 143: 527-39.
- 30. Soldner F, Hockemeyer D, Beard C, Gao Q, Bell GW, et al. (2009) Parkinson's disease patient-derived induced pluripotent stem cells free of viral reprogramming factors. Cell 136: 964-77.
- 31. Dimos JT, Rodolfa KT, Niakan KK, Weisenthal LM, Mitsumoto H, et al. (2008) Induced Pluripotent Stem Cells Generated from Patients with ALS Can Be Differentiated into Motor Neurons. Science 321: 1218-21.
- 32. Roy N, Mahadevan MS, McLean M, Shutter G, Yaraghi Z, et al. (1995) The gene for neuronal apoptosis inhibitory protein is partially deleted in individuals with spinal muscular atrophy. Cell 80: 167-78.
- 33. Seidl R, Bajo M, Böhm K, LaCasse EC, MacKenzie AE, et al. (1999) Neuronal apoptosis inhibitory protein (NAIP)-like immunoreactivity in brains of adult patients with Down syndrome. J Neural Transm Suppl 57: 283-91.
- 34. Christiea LA, Sua JH, Tua CH, Dicka MC, Zhoub J, et al. (2007) Differential regulation of inhibitors of apoptosis proteins in Alzheimer's disease brains. Neurobiol Dis 26: 165-73.
- 35. Xiao D, Wang J, Hampton LL, Weber HC (2001) The human gastrin-releasing peptide receptor gene structure, its tissue expression and promoter. Gene 264: 95-103.
- 36. Kamichi S, Wada E, Aoki S, Sekiguchi M, Kimura I, et al. (2005) Immunohistochemical localization of gastrin-releasing peptide receptor in the mouse brain. Brain Res 1032: 162-70.
- 37. Tchieu J, Kuoy E, Chin MH, Trinh H, Patterson M, et al. (2010) Female human iPSCs retain an inactive X chromosome. Cell Stem Cell 7: 329-42.
- 38. Roesler R, Luft T, Oliveira SH, Farias CB, Almeida VR, et al. (2006) Molecular mechanisms mediating gastrin-releasing peptide receptor modulation of memory consolidation in the hippocampus. Neuropharmacology 51: 350-7.
- 39. Lindsey JC, Lusher ME, Strathdee G, Brown R, Gilbertson RJ, et al. (2006) Epigenetic inactivation of MCJ (DNAJD1) in malignant paediatric brain tumours. Int J Cancer 118: 346-52.
- 40. Boettcher M, Kischkel F, Hoheisel JD (2010) High-definition DNA methylation profiles from breast and ovarian carcinoma cell lines with differing doxorubicin resistance. PLoS ONE 5: e11002.
- 41. Lister R, Pelizzola M, Dowen RH, Hawkins RD, Hon G, et al. (2009) Human DNA methylomes at base resolution show widespread epigenomic differences.
- 42. Maherali N, Sridharan R, Xie W, Utikal J, Eminli S, et al. (2007) Directly reprogrammed fibroblasts show global epigenetic remodeling and widespread tissue contribution. Cell Stem Cell 1: 55-70.
- 43. Yang J, Cai J, Zhang Y, Wang X, Li W, et al. (2010) Induced pluripotent stem cells can be used to model the genomic imprinting disorder Prader-Willi syndrome. I Biol Chem 285: 40303-11.
- 44. Hu BY, Weick JP, Yu J, Ma LX, Zhang XQ, et al. (2010) Neural differentiation of human induced pluripotent stem cells follows developmental principles but with variable potency. Proc Natl Acad Sci USA 107: 4335-40.

- 45. Feng Q, Lu SJ, Klimanskaya I, Gomes I, Kim D, et al. (2010) Hemangioblastic derivatives from human induced pluripotent stem cells exhibit limited expansion and early senescence. Stem Cells 28: 704-12.
- 46. Kaichi S, Hasegawa K, Takaya T, Yokoo N, Mima T, et al. (2010) Cell line-dependent differentiation of induced pluripotent stem cells into cardiomyocytes in mice. Cardiovasc Res 88: 314-23.
- 47. Crews L, Masliah E (2010) Molecular mechanisms of neurodegeneration in Alzheimer's disease. Hum Mol Genet 19: R12-20.
- 48. Jin ZB, Okamoto S, Osakada F, Homma K, Assawachananont J, et al. (2011) Modeling retinal degeneration using patient-specific induced pluripotent stem cells. PLoS ONE 6: e17084.
- 49. Wicklund L, Leão NR, Strömberg AM, Mousavi M, Hovatta O, et al. (2010) β-amyloid 1-42 oligomers impair function of human embryonic stem cell-derived forebrain cholinergic neurons. PLoS ONE 5: e15600.

Submit your next manuscript to Annex Publishers and benefit from:

- **Easy online submission process**
- Rapid peer review process
- > Online article availability soon after acceptance for Publication
- > Open access: articles available free online
- More accessibility of the articles to the readers/researchers within the field
- > Better discount on subsequent article submission

Submit your manuscript at http://www.annexpublishers.com/paper-submission.php